Published in final edited form as:
Pigment Cell Melanoma Res. 2012 January ; 25(1): 47–56. doi:10.1111/j.1755-148X.2011.00901.x.

Cellular and clinical report of new Griscelli syndrome type III cases

Wendy Westbroek[1], **Aharon Klar**[2], **Andrew R. Cullinane**[1], **Shira G Ziegler**[1], **Haggit Hurvitz**[2], **Ashraf Ganem**[2], **Kirkland Wilson**[1], **Heidi Dorward**[1], **Marjan Huizing**[1], **Haled Tamimi**[2], **Igor Vainshtein**[2], **Yackov Berkun**[3], **Moran Lavie**[3], **William A. Gahl**[1], and **Yair Anikster**[3]

[1]Section on Human Biochemical Genetics, Medical Genetics Branch, National Human Genome Research Institute, NIH, Bethesda MD, USA

[2]Department of Pediatrics, Bikur Cholim General Hospital, affiliated with the Hebrew University-Hadassah Medical School, Jerusalem, Israel

[3]Metabolic Disease Unit, Edmond and Lily Safra Children's Hospital, Sheba Medical Center, Tel Hashomer and Sackler School of Medicine Tel-Aviv University, Tel-Aviv, Israel

Summary

The RAB27A/Melanophilin/Myosin-5a tripartite protein complex is required for capturing mature melanosomes in the peripheral actin network of melanocytes for subsequent transfer to keratinocytes. Mutations in any one member of this tripartite complex cause three forms of Griscelli syndrome (GS), each with distinct clinical features but with a similar cellular phenotype. To date, only one case of GS type III (GSIII), caused by mutations in the *Melanophilin* (*MLPH)* gene, has been reported. Here we report seven new cases of GSIII in three distinct Arab pedigrees. All affected individuals carried a homozygous missense mutation (c.102C>T; p.R35W), located in the conserved Slp homology domain (SHD) of MLPH, and had hypomelanosis of the skin and hair. We report the first cellular studies on GSIII melanocytes, which demonstrated that MLPH(R35W) causes perinuclear aggregation of melanosomes in melanocytes, typical for GS. Additionally, co-immunoprecipitation assays showed that MLPH(R35W) lost its interaction with RAB27A, indicating pathogenicity of the R35W mutation.

Keywords

Griscelli syndrome type III; Melanophilin; melanocyte; melanosome; Myosin-5a; RAB27A; tripartite complex

INTRODUCTION

Pigment production in the epidermis of the skin and in hair follicles occurs in melanosomes, which are specialized lysosome-related organelles of melanocytes. Melanosomal pigment production takes place as the melanosome matures through defined, sequential morphological stages (Raposo and Marks, 2007). Mature melanosomes are transported within a melanocyte along microtubules to the cell periphery where they are captured in the cortical actin network before they are transferred to keratinocytes. The key player in peripheral melanosome capturing in the actin network is a tripartite complex containing the interacting proteins RAB27A, Myosin-5a (MYO5A), and Melanophilin (MLPH) (Huizing et

Address for correspondence and reprints: Wendy Westbroek, Ph.D., Medical Genetics Branch, National Human Genome Research Institute, National Institutes of Health, 35 Convent Drive, Building 35 Room 1A-209, Bethesda, MD 20892, USA. Phone: 301-451-0903, Fax: 301-402-6438, wwestbro@mail.nih.gov.

al., 2008; Van Gele et al., 2009). The distinct protein domains, interactions, interactors and proposed functions of these three proteins have been well described (Hume et al., 2007; Kuroda et al., 2003; Nagashima et al., 2002; Strom et al., 2002; Van Gele et al., 2009; Westbroek et al., 2003; Wu et al., 2002; Wu et al., 2005). Briefly, the small GTPase RAB27A in its GTP-bound form interacts with the melanosomal membrane, where it serves as a receptor for specific effectors. In melanocytes, membrane-bound RAB27A recruits its downstream effector MLPH. Subsequently, MLPH is able to bind actin, as well as the C-terminal globular tail domain of the actin-associated motor protein MYO5A, resulting in capturing of mature melanosomes in the peripheral actin network. Defects in any of the components of this tripartite complex result in failure to retain melanosomes in the cell periphery, resulting in perinuclear localization of melanosomes, and consequently failure to transfer melanosomes to neighboring keratinocytes, ultimately causing hypopigmentation. Mutations in the human genes encoding the tripartite protein complex cause different types of the rare autosomal recessive Griscelli syndrome (GS). The cellular hallmark of GS is perinuclear aggregation of melanosomes in melanocytes, resulting in skin hypomelanosis and a silvery-gray appearance to the hair (Van Gele et al., 2009). GS type I (GSI; MIM# 214450) is caused by mutations in the *MYO5A* gene on chromosome 15q21 (Pastural et al., 1997). Apart from hypopigmentation of the hair and skin, most GSI patients also suffer neurological impairment, except for patients with mutations in exon F of *MYO5A*, who are seemingly spared from the neurological symptoms (Menasche et al., 2003; Pastural et al., 1997). GS type II (GSII; MIM# 607624), the most common form of GS, is caused by mutations in *RAB27A* located on chromosome 15q21 (Menasche et al., 2000). Apart from mild hypopigmentation, GSII patients also suffer from immunological impairment due to malfunction in cytotoxic T lymphocyte granule release (Stinchcombe et al., 2004; Stinchcombe et al., 2001). GS type III (GSIII; MIM# 609227) is caused by mutations in *MLPH* located on chromosome 2q37.3 (Menasche et al., 2003). To date, only one GSIII patient has been reported, who carried a homozygous missense MLPH mutation, p.R35W; clinical characteristics of this patient were restricted to hypopigmentation of the skin and silvery-gray hair (Menasche et al., 2003). Here we describe three distinct Muslim-Arab pedigrees with clinical manifestations of GSIII, including hypopigmentation and silvery-gray hair. We diagnosed GSIII by identifying *MLPH* mutations in seven affected individuals. Detailed clinical, genetic and cellular studies are presented, including the first report of melanocyte studies in this rare subtype of Griscelli syndrome.

RESULTS

Case reports

The studied patients were part of three distinct highly consanguineous Muslim-Arab families (Figure 1), in which Griscelli syndrome was suspected by physicians who previously diagnosed Griscelli syndrome type II in a Muslim-Arab family (Hurvitz et al., 1993). Patient DB200 (Figure 2B) of Pedigree 1 was first referred to our clinic at the age of 4 years because of recurrent pneumonia but his immunological and neurological evaluation were normal. Upon visiting our clinic, abnormal pigmentation compared to his siblings (Figure 2A) was noticed, including silvery-gray hair, eyebrows, and eyelashes, which are typical clinical features for all three types of GS. Microscopic analysis of the silvery-gray hair from patients DB200 (Figure 2G) and DB212 (not shown) were comparable to silvery-gray hair from a previously described GS type II patient (Figure 2F) with reported mutations in *RAB27A* (Westbroek et al., 2008); irregular distributed pigment clumps were observed in both GSII and GSIII hairs (Figure 2F, G). As DB200 did not present with immune or neurological manifestations and the clinical phenotype was restricted to hypopigmentation, GS type III was considered.

Another Muslim-Arab family (Pedigree 2) with 4 silvery-gray hair patients came to our attention. Apart from hypopigmentation and silvery-gray hair, two patients from Pedigree 2, DB213 (Figure 2D) and DB250 (not shown) showed no other clinical features. However, two other patients of this highly consanguineous family, DB212 (Figure 2C) and DB252 (not shown), had additional clinical anomalies. Patient DB252 suffered from psychomotor retardation while DB212 had marfanoid status; these features may be related to defects in other gene(s) and is beyond the scope of this paper.

Both patients of Pedigree 3, DB275 and DB273, only manifested with hypopigmentation and silvery-gray hair (data not shown); no additional clinical features were observed. A summary of the clinical features of the patients from the three presented pedigrees is given in Table 1.

DB200 and DB212 melanocytes show a cellular Griscelli-like phenotype

We performed light and immuno-fluorescence confocal microscopy to study the distribution of melanosomes in melanocytes of patients DB200 and DB212. Light microscopy showed that control melanocytes had a peripheral distribution of melanosomes throughout the cell with accumulation in the dendritic tips (Figure 3A enlarged in 3B, arrwos). In both DB200 and DB212 melanocytes, the typical cellular phenotype of GS, which is characterized by perinuclear accumulation of melanosomes, was observed (Figure 3E enlarged in 3F, 3I enlarged in 3J, arrowheads) while the dendrites and dendritic tips were devoid of pigment (arrows). Next, we used laser scanning confocal microscopy to evaluate the localization of the melanosome-specific protein PMEL17 (Figure 3C, D, G, H, K, L). PMEL17 is the protein responsible for formation of melanosomal striations for melanin deposition and is detected by the HMB45 antibody (Theos et al., 2005). HMB45 staining showed a punctate pattern in the cell periphery and dendrites, with a concentration in the dendritic tips in control melanocytes (Figure 3C, enlarged 3D, arrows), while HMB45 staining in DB200 and DB212 cells showed a perinuclear accumulation (Figure 3G enlarged in 3H, 3K enlarged in 3L, arrowheads); no pigment was observed in dendrites or dendritic tips (arrows). The laser scanning confocal microsocpy data is consistent with the observations made for melanosome distribution using light microscopy.

MLPH is mutated in the affected patients

Since the affected patients had clinical characteristics of GSIII and their melanocytes showed a perinuclear accumulation of melanosomes typical of GS (Huizing et al., 2008; Menasche et al., 2003; Van Gele et al., 2009), mutation analysis of *MLPH* was performed. Sequence analyses of all 13 exons of *MLPH* of patients DB200 (Figure 1A, Pedigree 1) and DB212 (Figure 1B, Pedigree 2) revealed a homozygous missense mutation (c.102C>T; p.R35W) in exon 2 of the *MLPH* gene in both patients, no other variants were detected. Further familial analysis revealed that in Pedigree 1, DB201 (father), DB202 (mother), DB215, DB216, DB217, DB218, and DB219 were carriers for the *MLPH* mutation (Figure 1A). In pedigree 2, DB212, DB213, DB250, and DB252, clinically diagnosed with GSIII, were all homozygous for *MLPH* (c.102C>T; p.R35W), while DB214, DB247, DB248, and DB251 were all carriers; DB249 was not a carrier (Figure 1B). In pedigree 3, DB273 and DB275, both clinically diagnosed with GSIII, were homozygous for *MLPH* (c.102C>T; p.R35W), while DB274 was a carrier (Figure 1C). Since GSII patients with mutations in Exon F of *MYO5A* can mimic the phenotype of GSIII patients (Menasche et al., 2003), and we identified a missense mutation in MLPH, we decided to sequence all affected individuals for this exon and flanking intronic sequence. This identified no changes in any individual (data not shown), further suggesting that the mutation in *MLPH* is pathogenic.

MLPH protein is downregulated in GSIII melanocytes

Molecular confirmation of a MLPH mutation prompted us to further analyze the expressed *MLPH* mRNA and MLPH protein levels in melanocytes. Quantitative real time PCR revealed a minor, but statistically significant, difference in relative *MLPH* mRNA expression of GSIII cells (83.14 ± 1.69% for DB200 and 83.48 ± 1.02% for DB212) compared to control (100 ± 1.52%). *MYO5A* or *RAB27A* mRNA levels were similar between GSIII (97.84 ± 2.30% and 98.56% ± 2.16% for *MYO5A*; 97.84 ± 3.18% and 93.24 ± 3.64%) and control (Figure 4A). For all qRT-PCR, values shown are mean values ± 1 SEM from 3 independent assays for each gene. Since *RAB27A* has a homologue, *RAB27B* (Chen et al., 1997), we tested whether this became up-regulated in GSIII patient melanocytes as a potential compensatory mechanism. *RAB27B* mRNA could not be detected in either control or GSIII patient melanocytes, despite our assay detecting expression in breast tissue (data not shown), suggesting that upregulation of RAB27B did not occur.

Western blot analysis of the protein levels of the members of the tripartite complex on protein lysates from control, DB200, and DB212 melanocytes showed that MLPH protein expression is nearly absent in both GSIII melanocytes lysates (0.65% for DB200 and 3.61% for DB212) compared to control (100%) (Figure 4B). In DB200, both MYO5A (21.06%) and RAB27A (63.17%) levels were decreased (Figure 4B), while in DB212 levels for both MYO5A (152.63%) and RAB27A (226.82%) were increased (Figure 4B). Similar to mRNA expression, RAB27B protein was not expressed in control or GSIII melanocytes (data not shown). Significant decreased MLPH (green) was confirmed at the cellular level for DB200 for which the imaged field had a mean intensity of 3 (Figure 4B, b) compared to control melancoytes with a mean intensity of 6 (Figure 4B, f) by confocal laser scanning microscopy.

MLPH(R35W) induces a cellular Griscelli phenotype in melanocytes

We showed that the amount of mutated MLPH protein expressed in GSIII melanocytes was decreased (Figure 4), however, this did not demonstrate pathogenecity of the MLPH p.R35W mutation. It was previously described that murine *leaden* melanocytes exhibit a clustered perinuclear distribution of melanosomes that was recapitulated when mutant MLPH was over-expressed in control melanocytes (Menasche et al., 2003). To study whether MLPH(R35W) is the GSIII disease causing mutation, we electroporated control melanocytes with DsRed-MLPH(WT) (Figure 5A) or DsRed-MLPH(R35W) (Figure 5B). Laser scanning confocal microscopy was used to evaluate the distribution of the melanosome-specific protein PMEL17 (HMB45) in these electorporated cells. In control melanocytes over-expressing DsRed-MLPH(WT), both HMB45 and DsRed-MLPH(WT) showed a punctate pattern throughout the cell body and dendrites, with accumulation and co-localization in dendritic tips (Figure 5A, arrow, insert). In control melanocytes over-expressing DsRed-MLPH(R35W) (Figure 5B, red), PMEL17 (Figure 5B, green) accumulated in the perinuclear area and was absent from the dendrites and dendritic tips (Figure 5B, arrow, insert), similar to the melanosome distribution described for *leaden* melanocytes (Matesic et al., 2001; Menasche et al., 2003). Next, we investigated whether the perinuclear accumulation of melanosomes in GSIII melanocytes could be rescued by over-expressing wild type MLPH in GSIII cells. DB212 melanocytes transfected with DsRed-MLPH(WT) (Figure 5C, asterisk) showed that both PMEL17 (Figure 5C, green) and DsRed-MLPH(WT) (Figure 5C, red) showed a vesicular pattern and co-localization in the cell periphery and in dendrites with accumulation in dendritic tips (Figure 5C, insert), while non-transfected melanocytes showed the typical accumulation of PMEL17 in the perinuclear region (Figure 5C, arrows). DB212 melanocytes transfected with DsRed-MLPH(R35W), showed no rescue of PMEL17 localization to the cell periphery, instead PMEL17 remained

localized in the perinuclear region (Figure 5D, arrow) while dendrites and tips remained devoid of the HMB45 marker (Figure 5D, arrowheads). Interestingly, both wild type and MLPH(R35W) localized to the periphery of the cell (Figure 5, red), suggesting that MLPH(R35W) is able to interact with actin but not with melanosomes.

MLPH(R35W) does not interact with RAB27A

In melanocytes, the MLPH protein is recruited to melanosome-associated GTP-bound RAB27A. To study the protein-protein interaction between MLPH(R35W) and RAB27A, we performed a co-immunoprecipitation assay (co-IP). Protein extracts were made from HEK cells transfected with GFP-RAB27A(WT) and either DsRed-MLPH(WT) or DsRed-MLPH(R35W). The co-IP assays were performed with anti-GFP antibodies and the Western blots were probed with anti-MLPH, anti-GFP, or anti-RAB27A antibodies (Figure 6). DsRed-MLPH(WT) and DsRed-MLPH(R35W) protein expression in HEK cells was comparable (Figure 6, input). MLPH(WT) co-immunoprecipitated with RAB27A(WT) (Figure 6, lane 1) while DsRed-MLPH(R35W) did not (Figure 6, lane 2). These data indicate that the conserved R35 amino acid of MLPH is important in binding the small GTPase RAB27A.

DISCUSSION

To date, only one disease-causing *MLPH* homozygous missense mutation (c.102C>T; p.R35W) has been described in a French GSIII patient of Turkish origin ((Menasche et al., 2003); Dr. Genevieve de Saint Basile, personal communication). In this patient, clinical characteristics were restricted to hypopigmentation of the skin and hair with no additional clinical phenotype. In the current study, three distinct Muslim-Arab pedigrees are presented that included patients with typical GSIII manifestations of the hair and skin; the pedigrees came to our attention because of other non-Griscelli related clinical manifestations, probably due to the high consanguinity in the families (Figure 1). All the GSIII subjects in the current study were homozygous for the previously described (c.102C>T; p.R35W) mutation (Menasche et al., 2003). Mutations in exon F of *MYO5A*, which can also cause a GSIII phenotype (Menasche et al., 2003), were not detected in any of the pedigrees. Interestingly, the same R35W mutation in MLPH was found to cause the coat color dilution of the *lavender* chicken, resulting in defects in transfer of melanosomes into the keratinocytes of the growing feather (Vaez et al., 2008). In the *leaden* mouse, the murine homologue of GSIII, R35 is one of the highly conserved amino acids deleted, resulting from a 21-bp *Mlph* mutation (Matesic et al., 2001). The highly conserved R35 amino acid residue is located in the N-terminal Slp homology domain (SHD), which is involved in binding members of the RAB27 family (Kuroda et al., 2005). We showed that MLPH(R35W) did not interact with RAB27A (Figure 6); these data are consistent with previous findings in the originally described GSIII patient (Menasche et al., 2003), suggesting that R35 is a crucial amino acid in the N-terminal SHD domain of MLPH. It has been established that the C-terminal part of MLPH is involved in direct binding with actin (Kuroda et al., 2003); we showed that over-expressed MLPH(R35W) was still able to localize to the actin-rich cell periphery (Figure 5B, D) suggesting that the mutation does not disrupt the binding of mutated MLPH to actin. The effect of the R35W amino acid substitution on the endogenous level of MLPH protein was not previously studied. Here, we show that the endogenous levels of *MLPH* mRNA in GSIII melanocytes were slightly down-regulated (Figure 4A) but this is not indicative of mRNA instability. Also note that since only one control sample was used, it is not established what the endogenous variation of *MLPH* expression is between controls. MLPH protein levels were much lower in both GSIII melanocytes (0.65% for DB200 and 3.61% for DB212) compared to control melanocytes (100%) (Figure 4B). This might suggest that the R35W amino acid substitution has a negative effect on the protein stability of MLPH. The

data presented here strongly suggests that the cellular phenotype in melanocytes is caused by the R35W mutation. This was demonstrated by the induction of perinuclear accumulation of melanosomes by over-expression of MLPH(R35W) in control melanocytes (Figure 5B), while over-expression of MLPH(R35W) in GSIII melanocytes failed to rescue perinuclear melanosome distribution (Figure 5D). Although this does not rule out that low endogenous levels of mutant MLPH by itself could contribute to the cellular phenotype in GSIII melanocytes. One way to test this would be to express MLPH(WT) at comparable low levels as the endogenous mutant MLPH and measure rescue of the cellular phenotype in melanocytes. Please note that in our rescue experiments, we imaged GSIII melanocytes that showed the lowest DsRed signal (Figure 5C, 5D). In addition, we showed that MYO5A and RAB27A protein levels were decreased in GSIII melanocytes derived from patient DB200, while MYO5A and RAB27A levels were up-regulated in melanocytes derived from patient DB212 (Figure 4). For DB200, this is consistent with a previous study done by Hume and colleagues (2007), where specific siRNA's were used against each member of the tripartite complex in mouse melan-a cells, while the expression levels of the non-silenced tripartite members were monitored after 72 hours. Silencing of MLPH down-regulated protein levels of MYO5A and RAB27A (Hume et al., 2007). For patient DB212 this was not the case. Data discrepancies between DB200 and DB212 might be because of other affected genes, due to high consanguinity, that might play a role in tri-partite complex protein regulation and/or stability. Also, note that Hume and colleagues used artificial siRNA's to silence *MLPH* mRNA in immortalized mouse melan-a melanocytes (Hume et al., 2007), while the current study investigated primary human melanocytes with a naturally occurring MLPH mutation which did show significant down-regulation in protein levels but not in mRNA levels. No expression of RAB27B at the mRNA or protein level was detected for patient DB200 and DB212 (data not shown).

In conclusion, we showed an in depth cellular analysis of GSIII melanocytes and biochemical analysis of the MLPH(R35W) protein. Importantly, we show that the R35W mutation is disease causing. However, it is currently too soon to state that MLPH(R35W) could be a hot spot for mutations in the Middle Eastern population or the mutation is perhaps more widespread. To determine this more patients need to be diagnosed, however, since the clinical phenotype of GSIII patients is restricted to only hypopigmentation of the skin and silvery-gray hair, it is hard to identify new patients. Most families may only come to the clinician's attention because of non-related GSIII clinical manifestations, leading to the under diagnosis of this subtype of GS.

METHODS

Patients and cells

Two families with affected GSIII patients were enrolled in clinical protocol 76-HG-0238, "Diagnosis and Treatment of Inborn Errors of Metabolism" (http://clinicaltrials.gov), approved by the NHGRI Institutional Review Board. Written informed consent was obtained from the patients or parents of patients. A skin biopsy was obtained from affected patients DB200 (Pedigree 1) and DB212 (Pedigree 2), and primary epidermal melanocytes were cultured. Briefly, a forearm skin biopsy was washed in phosphate buffered saline (PBS) and incubated for 2 hours in trypsin at 37°C. The biopsy was vortexed until detachment of the epidermal layer was visible. Pieces of epidermal layer were then transferred to a 6-well dish in melanocyte culture medium consisting of Ham's F10 (Invitrogen, Carlsbad, CA), 5% fetal calf serum (Gemini Bio-Products, West Sacramento, CA), 5 μg/L basic fibroblast growth factor (Sigma, St. Louis, MO), 10 μg/L Endothelin (Sigma), 7.5 mg/L 3-Isobutyl-1-methylxanthine (Sigma), 30 μg/L Choleratoxin (Sigma), 3.3 μg/L Phorbol 12-myristate 13-acetate (Sigma), 10 ml Pen/Strep/Glutamine (Invitrogen) and 1 ml Fungizone (Invitrogen). Fibroblasts growth in the melanocyte culture was prevented by

treatment with 100 μg/ml Geneticin in melanocyte medium for 3 days (Halaban and Alfano, 1984). All melanocyte cultures were tested for purity with the mouse monoclonal melanocyte specific HMB45 antibody (Lab Vision, Fremont, CA; 1:100 dilution) by immuno-fluorescence laser scanning confocal microscopy. Control human primary epidermal melanocytes were purchased from Cascade Biologics (Portland, OR). Human Embryonic Kidney (HEK) cells (gift of Dr. Jan Tavernier, Ghent University, Belgium) were cultured in Dulbecco's modi ed Eagle's medium (DMEM; Invitrogen) and 10% fetal bovine calf serum (Gemini Bio-Products).

Mutation analysis

Genomic DNA was isolated from whole blood using the Puregene DNA purification kit according to the manufacturer's guidelines (Gentra Systems, Minneapolis, Minnesota). Sequencing of the 13 *MLPH* coding exons and their intron–exon junctions as well as the *MYO5A* exon F coding exon was carried out. Briefly, a touchdown PCR was performed in a final volume of 10μL containing 50ng of genomic DNA, 3μM of sense and antisense M13-tagged *MLPH* primers (primer sequences available upon request), and 5μl of HotStar Master Mix (Qiagen, Valencia, CA). The PCR products were purified using ExoSap (USB, Cleveland, OH) for 45min at 37°C and subjected to a sequencing PCR with M13 primers by using the Big Dye terminator kit (v3.1; Applied Biosystems, Foster City, CA). Linear amplification products were then separated in an automated capillary sequencer (ABI PRISM 3130×l Genetic Analyzer, Applied Biosystems). Sequences were compared to reference sequences for *MLPH* (ENST00000264605) and *MYO5A* exon F (GenBank AF090424.1) using Sequencher software 4.8.

RNA isolation and quantitative Real time PCR

Total RNA from control, DB200 and DB212 melancoytes was isolated using the Trizol reagent (Invitrogen) according to the manufacturer's protocol. Cell extracts were filtered over a Qiashredder column to eliminate melanin (Qiagen, Valencia, CA). RNA was treated with a DNase kit (DNA-free) according to the manufacturer's protocol (Applied Biosystems, Austin, TX). RNA concentration and purity were measured on the Nanodrop ND-1000 (Nanodrop Technologies, Wilmington, DE). First-strand cDNA was synthesized using a high-capacity RNA-to-cDNA kit (Applied Biosystems) according to the manufacturer's guidelines. Absence of gDNA contamination was verified with a standard primer pair for beta-actin (ACTB). Quantitative real-time PCR was performed using 100 ng of cDNA, Taqman gene expression master mix reagent, and Assays-On-Demand (Applied Biosystems) for *MLPH* (Assay ID Hs00225445_m1), *MYO5A* (Assay ID Hs00165309_m1), *RAB27A* (Assay ID Hs00608302_m1), *RAB27B* (Assay ID Hs00188156_m1) and a control gene, *GAPDH* (Assay ID Hs99999905_m1), on an ABI PRISM 7900 HT Sequence Detection System (Applied Biosystems) using the comparative CT method (ΔΔCT). The cycling conditions were 2 minutes at 50 °C, 10 minutes at 95 °C, and 40 cycles at 95 °C for 15 seconds and 60°C for 60 seconds. It is known that *RAB27B* is not expressed in control melanocytes (Westbroek et al., 2004); as a positive control for *RAB27B* expression, we used a previously described human breast cancer sample (Hendrix et al., 2010b).

Plasmids, mutagenesis and electroporation

The human *MLPH* (c.102C>T; p.R35W) mutant was generated by PCR-based site-directed mutagenesis using the Quickchange mutagenesis kit according to the manufacturer's guidelines (Stratagene, La Jolla, CA), using the previously described DsRed-MLPH(WT) plasmid (Westbroek et al., 2008) as a template and the following mutagenesis primers: forward: CGAAGGAAAGAAGAGGAATGGCTAGAGGCGTTGAAG; reverse: CTTCAACGCCTCTAGCCATTCCTCTTCTTTCCTTCG. A previously described GFP-

RAB27A(WT) plasmid was used for co-immunoprecipitation (Westbroek et al., 2008). Electroporation of the various cell types was performed in a Nucleofector electroporator, according to the manufacturer's guidelines (Lonza, Walkersville, MD). A mixture of 100 μL Nucleofector solution and plasmid DNA was added to approximately 700,000 melanocytes (1 μg plasmid DNA, U_16 Nucleofector program) or HEK cells (5 μg plasmid DNA, Q_01 Nucleofector program).

Bright field microscopy

Bright field images of hair and primary melanocytes were obtained using a Zeiss Axiovert 200M with a Plan NeoFluar 40X/1.3 oil DIC objective. Images were obtained with an Axiocam HRc color camera with Axiovision software version 4.5.0 (Carl Zeiss, Microimaging Inc., Thornwood, NY, USA).

Laser scanning confocal microscopy

Control or GSIII melanocytes (DB200 and DB212) non-electroporated or electroporated with DsRed-MLPH(WT) or DsRed-MLPH(R35W) were grown for 48h on glass slides. The cells were fixed in 3% paraformaldehyde, blocked in PBS containing 0.1% saponin, 100 μM glycine, and 2% donkey serum followed by incubation with the HMB45 mouse monoclonal antibody (Lab Vision, Fremont, CA) (1:100 dilution) or the MLPH rabbit polyclonal antibody (Proteintech Group Inc, Chicago, IL) (1:50 dilution). Cells were co-stained with BODIPY 555 phalloidin to visualize the cell boundaries (Invitrogen). The cells were washed and incubated with donkey anti-mouse or rabbit secondary antibodies conjugated to ALEXA-488 (Invitrogen), washed again, and mounted in VectaShield plus DAPI (Vector Laboratories, Burlingame, CA). Cells were imaged with a Zeiss 510 META confocal laser-scanning microscope (Carl Zeiss, Microimaging Inc.) using a 488 argon and a 543 HeNe laser. Images were acquired using a Plan NeoFluar 40X/1.3 oil DIC objective. All images are shown as collapsed z-stacks.

Co-immunoprecipitation

Twenty hours after transfection of HEK cells with GFP-RAB27A(WT) or DsRed-MLPH(R35W) or DsRed-MLPH(WT), cells were washed with PBS and lysed in lysis buffer, consisting of 1% Nonidet P40, 50 mM Tris pH 8, 150 mM NaCl and a protease inhibitor mix (Roche Diagnostics, Indianapolis, IN). Mouse monoclonal anti-GFP (Millipore, Billerica, MA) was coupled to M-280 magnetic dynabeads (Invitrogen) and mixed with cell extracts in lysis buffer. After overnight incubation, the beads were washed six times in lysis buffer and boiled in Laemmli buffer (Biorad, Hercules, CA) for 5min. Entire eluates were loaded onto a 4–12 % Tris-Glycine gel (Invitrogen) for Western blotting.

Western blotting

Equivalent amounts of total protein, as determined by BCA assay (Pierce Biotechnology, Rockford, IL), from HEK cells or control and patient melanocyte extracts, were loaded onto 4–12 % Tris-Glycine gels. After blotting, the nitrocellulose membranes (Invitrogen) were probed with a rabbit polyclonal antibody specific for RAB27B (Barral et al., 2002), a mouse monoclonal antibody specific for RAB27A (BD Biosciences, San Jose, CA; (Hendrix et al., 2010a), a mouse monoclonal α-tubulin antibody (loading control, Sigma), a GFP mouse monoclonal antibody (Millipore), a mouse monoclonal MYO5A antibody (Sigma) and a rabbit polyclonal MLPH antibody (Proteintech Group Inc.), Followed by incubation with HRP-labeled secondary anti-mouse or anti-rabbit antibodies (Amersham Biosciences, Piscataway, NJ). The antigen-antibody complexes were detected with an Enhanced Chemiluminescence (ECL) kit (Amersham Biosciences). Relative quantification of protein

amount was performed with ImageJ free software (NIH, Bethesda, Maryland). Tubulin was used as the internal control for normalization.

Acknowledgments

We kindly acknowledge the patients and their families who participated in this study. This research was supported by the Intramural Research Program of the National Human Genome Research Institute, National Institutes of Health, Bethesda, Maryland, USA.

References

Barral DC, Ramalho JS, Anders R, Hume AN, Knapton HJ, Tolmachova T, Collinson LM, Goulding D, Authi KS, Seabra MC. Functional redundancy of Rab27 proteins and the pathogenesis of Griscelli syndrome. J Clin Invest. 2002; 110:247–57. [PubMed: 12122117]

Chen D, Guo J, Miki T, Tachibana M, Gahl WA. Molecular cloning and characterization of rab27a and rab27b, novel human rab proteins shared by melanocytes and platelets. Biochem Mol Med. 1997; 60:27–37. [PubMed: 9066979]

Halaban R, Alfano FD. Selective elimination of fibroblasts from cultures of normal human melanocytes. In Vitro. 1984; 20:447–50. [PubMed: 6724622]

Hendrix A, Braems G, Bracke M, Seabra M, Gahl W, De Wever O, Westbroek W. The secretory small GTPase Rab27B as a marker for breast cancer progression. Oncotarget. 2010a; 1:304–8. [PubMed: 21304180]

Hendrix A, Maynard D, Pauwels P, Braems G, Denys H, Van Den Broecke R, Lambert J, Van Belle S, Cocquyt V, Gespach C, et al. Effect of the secretory small GTPase Rab27B on breast cancer growth, invasion, and metastasis. J Natl Cancer Inst. 2010b; 102:866–80. [PubMed: 20484105]

Huizing M, Helip-Wooley A, Westbroek W, Gunay-Aygun M, Gahl WA. Disorders of lysosome-related organelle biogenesis: clinical and molecular genetics. Annu Rev Genomics Hum Genet. 2008; 9:359–86. [PubMed: 18544035]

Hume AN, Ushakov DS, Tarafder AK, Ferenczi MA, Seabra MC. Rab27a and MyoVa are the primary Mlph interactors regulating melanosome transport in melanocytes. J Cell Sci. 2007; 120:3111–22. [PubMed: 17698919]

Hurvitz H, Gillis R, Klaus S, Klar A, Gross-Kieselstein F, Okon E. A kindred with Griscelli disease: spectrum of neurological involvement. Eur J Pediatr. 1993; 152:402–5. [PubMed: 8319705]

Kuroda TS, Ariga H, Fukuda M. The actin-binding domain of Slac2-a/melanophilin is required for melanosome distribution in melanocytes. Mol Cell Biol. 2003; 23:5245–55. [PubMed: 12861011]

Kuroda TS, Itoh T, Fukuda M. Functional analysis of slac2-a/melanophilin as a linker protein between Rab27A and myosin Va in melanosome transport. Methods Enzymol. 2005; 403:419–31. [PubMed: 16473608]

Matesic LE, Yip R, Reuss AE, Swing DA, O'sullivan TN, Fletcher CF, Copeland NG, Jenkins NA. Mutations in Mlph, encoding a member of the Rab effector family, cause the melanosome transport defects observed in leaden mice. Proc Natl Acad Sci U S A. 2001; 98:10238–43. [PubMed: 11504925]

Menasche G, Ho CH, Sanal O, Feldmann J, Tezcan I, Ersoy F, Houdusse A, Fischer A, De Saint Basile G. Griscelli syndrome restricted to hypopigmentation results from a melanophilin defect (GS3) or a MYO5A F-exon deletion (GS1). J Clin Invest. 2003; 112:450–6. [PubMed: 12897212]

Menasche G, Pastural E, Feldmann J, Certain S, Ersoy F, Dupuis S, Wulffraat N, Bianchi D, Fischer A, Le Deist F, et al. Mutations in RAB27A cause Griscelli syndrome associated with haemophagocytic syndrome. Nat Genet. 2000; 25:173–6. [PubMed: 10835631]

Nagashima K, Torii S, Yi Z, Igarashi M, Okamoto K, Takeuchi T, Izumi T. Melanophilin directly links Rab27a and myosin Va through its distinct coiled-coil regions. FEBS Lett. 2002; 517:233–8. [PubMed: 12062444]

Pastural E, Barrat FJ, Dufourcq-Lagelouse R, Certain S, Sanal O, Jabado N, Seger R, Griscelli C, Fischer A, De Saint Basile G. Griscelli disease maps to chromosome 15q21 and is associated with mutations in the myosin-Va gene. Nat Genet. 1997; 16:289–92. [PubMed: 9207796]

Raposo G, Marks MS. Melanosomes--dark organelles enlighten endosomal membrane transport. Nat Rev Mol Cell Biol. 2007; 8:786–97. [PubMed: 17878918]

Stinchcombe J, Bossi G, Griffiths GM. Linking albinism and immunity: the secrets of secretory lysosomes. Science. 2004; 305:55–9. [PubMed: 15232098]

Stinchcombe JC, Barral DC, Mules EH, Booth S, Hume AN, Machesky LM, Seabra MC, Griffiths GM. Rab27a is required for regulated secretion in cytotoxic T lymphocytes. J Cell Biol. 2001; 152:825–34. [PubMed: 11266472]

Strom M, Hume AN, Tarafder AK, Barkagianni E, Seabra MC. A family of Rab27-binding proteins. Melanophilin links Rab27a and myosin Va function in melanosome transport. J Biol Chem. 2002; 277:25423–30. [PubMed: 11980908]

Theos AC, Truschel ST, Raposo G, Marks MS. The Silver locus product Pmel17/gp100/Silv/ME20: controversial in name and in function. Pigment Cell Res. 2005; 18:322–36. [PubMed: 16162173]

Vaez M, Follett SA, Bed'hom B, Gourichon D, Tixier-Boichard M, Burke T. A single point-mutation within the melanophilin gene causes the lavender plumage colour dilution phenotype in the chicken. BMC Genet. 2008; 9:7. [PubMed: 18197963]

Van Gele M, Dynoodt P, Lambert J. Griscelli syndrome: a model system to study vesicular trafficking. Pigment Cell Melanoma Res. 2009; 22:268–82. [PubMed: 19243575]

Westbroek W, Lambert J, Bahadoran P, Busca R, Herteleer MC, Smit N, Mommaas M, Ballotti R, Naeyaert JM. Interactions of human Myosin Va isoforms, endogenously expressed in human melanocytes, are tightly regulated by the tail domain. J Invest Dermatol. 2003; 120:465–75. [PubMed: 12603861]

Westbroek W, Lambert J, De Schepper S, Kleta R, Van Den Bossche K, Seabra MC, Huizing M, Mommaas M, Naeyaert JM. Rab27b is up-regulated in human Griscelli syndrome type II melanocytes and linked to the actin cytoskeleton via exon F-Myosin Va transcripts. Pigment Cell Res. 2004; 17:498–505. [PubMed: 15357836]

Westbroek W, Tuchman M, Tinloy B, De Wever O, Vilboux T, Hertz JM, Hasle H, Heilmann C, Helip-Wooley A, Kleta R, et al. A novel missense mutation (G43S) in the switch I region of Rab27A causing Griscelli syndrome. Mol Genet Metab. 2008; 94:248–54. [PubMed: 18397837]

Wu XS, Rao K, Zhang H, Wang F, Sellers JR, Matesic LE, Copeland NG, Jenkins NA, Hammer JA 3rd . Identification of an organelle receptor for myosin-Va. Nat Cell Biol. 2002; 4:271–8. [PubMed: 11887186]

Wu XS, Tsan GL, Hammer JA 3rd . Melanophilin and myosin Va track the microtubule plus end on EB1. J Cell Biol. 2005; 171:201–7. [PubMed: 16247022]

Significance

This is the first report of Griscelli syndrome type III (GSIII) in Arab pedigrees as well as a thorough cellular and biochemical study of epidermal GSIII melanocytes. All seven patients carried the same, previously reported, amino acid substitution in melanophilin (MLPH): p.R35W. We showed that, although endogenous levels of MLPH were significantly decreased in GSIII melanocytes, the pathologic defect came from the R35W substitution, which induced aggregation of melanosomes in the perinuclear area of melanocytes due to failure to interact with RAB27A.

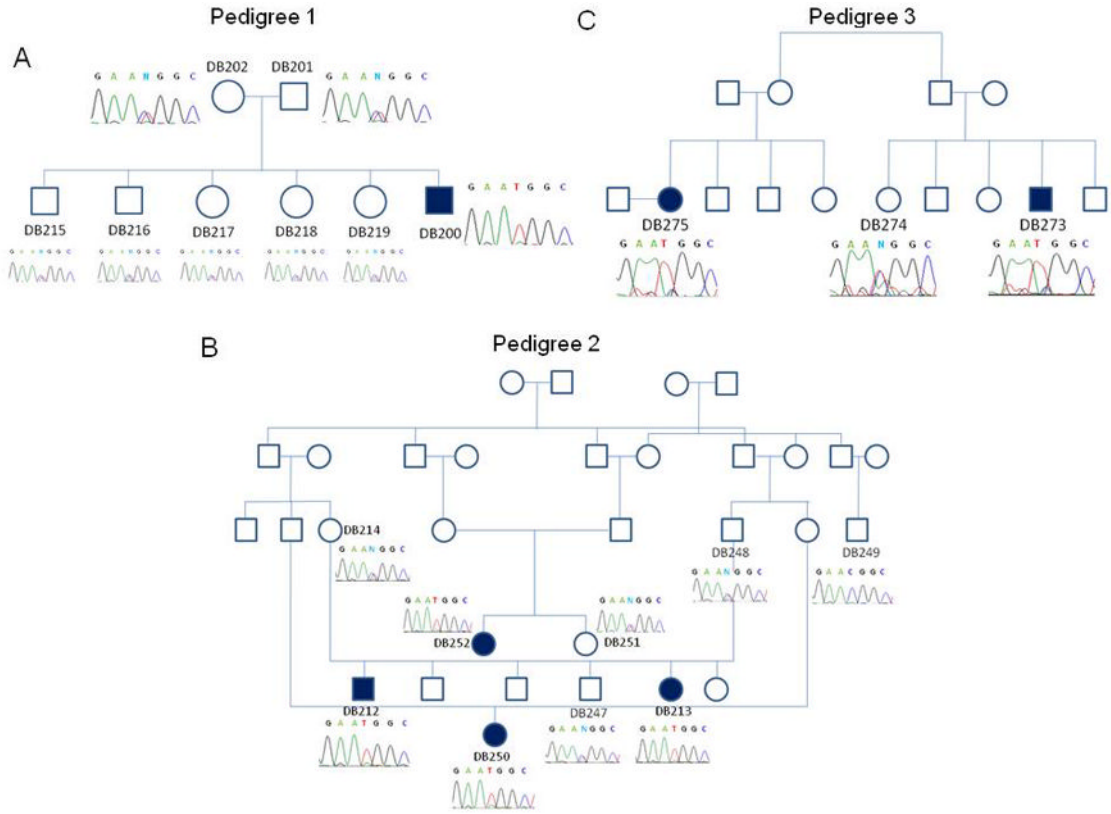

Figure 1. The three studied Muslim-Arab pedigrees with GSIII

(A) All members of Pedigree 1 were heterozygous for *MLPH* (c.102C>T; p.R35W), except for the clinically diagnosed GSIII patient DB200, who is homozygous. (B) In Pedigree 2, DB214, DB247, DB248, and DB251 are heterozygous for (c.102C>T; p.R35W) while DB212, DB213, DB250 and DB252, all diagnosed clinically with GSIII, are homozygous. (C) In Pedigree 3, patients DB273 and DB275 are homozygous while DB274 is heterozygous for *MLPH* (c.102C>T; p.R35W).

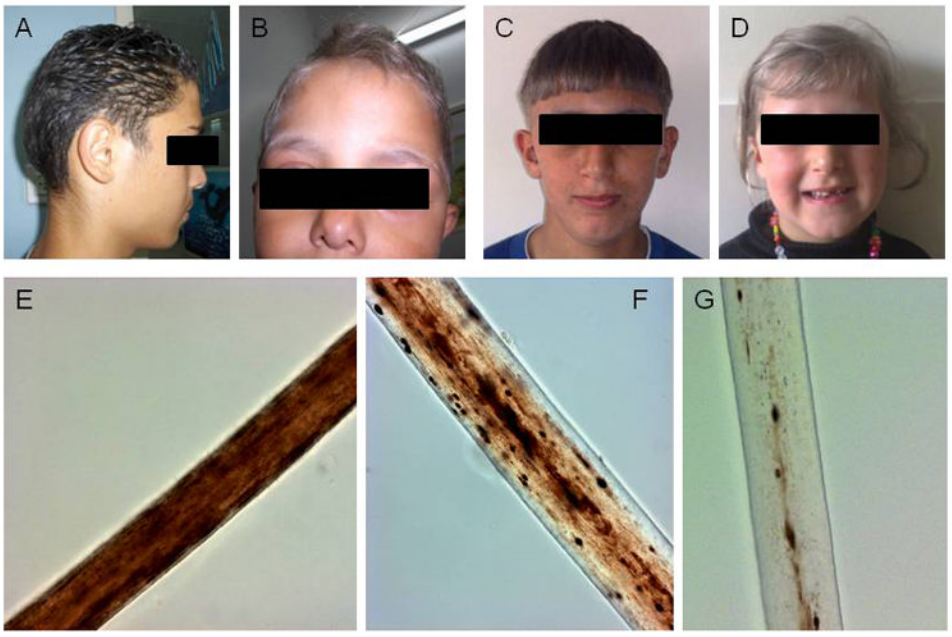

Figure 2. Hair and skin phenotypes of GSIII patients

(A) Non-affected sibling of DB200 with dark hair and skin. GSIII patients DB200 (B), DB212 (C) and DB213 (D) with light pigmented skin and silvery-gray hair. (E) Control dark hair with evenly distributed pigment in the hair shaft. (F) Silvery-gray hair of a GSII patient with a RAB27A mutation showing pigment clumping in the hair shaft. (G) Silvery-gray hair of GSIII patient DB200 showing pigment clumps in the hair shaft.

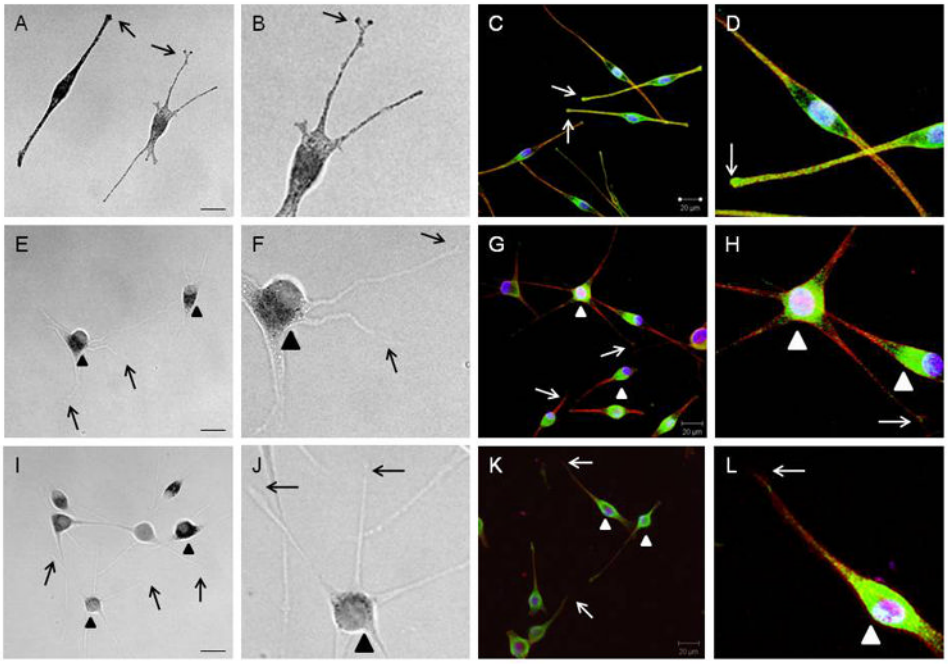

Figure 3. Distribution of melanosomes in control and GSIII melanocytes

Bright field microscopy of control melanocytes showing accumulation of pigmented melanosomes in the dendritic tips (A,B, arrows) and perinuclear accumulation in melanocytes from DB200 (E,F, arrowheads) and DB212 (I,J, arrowheads) with dendritic tips devoid of pigment (E,F,I,J, arrows). Staining for the melanosome-specific marker PMEL17 (green), actin (red) and nucleus (blue) shows cellular distribution of melanosomes with accumulation in dendritic tips in control melanocytes (C,D, arrows), while GSIII melanocytes DB200 (G,H) and DB212 (K,L) show melanosomal accumulation in the perinuclear area (arrowheads) with the dendritic extensions are devoid of melanosomes (arrows). Scale bar = 20 μm.

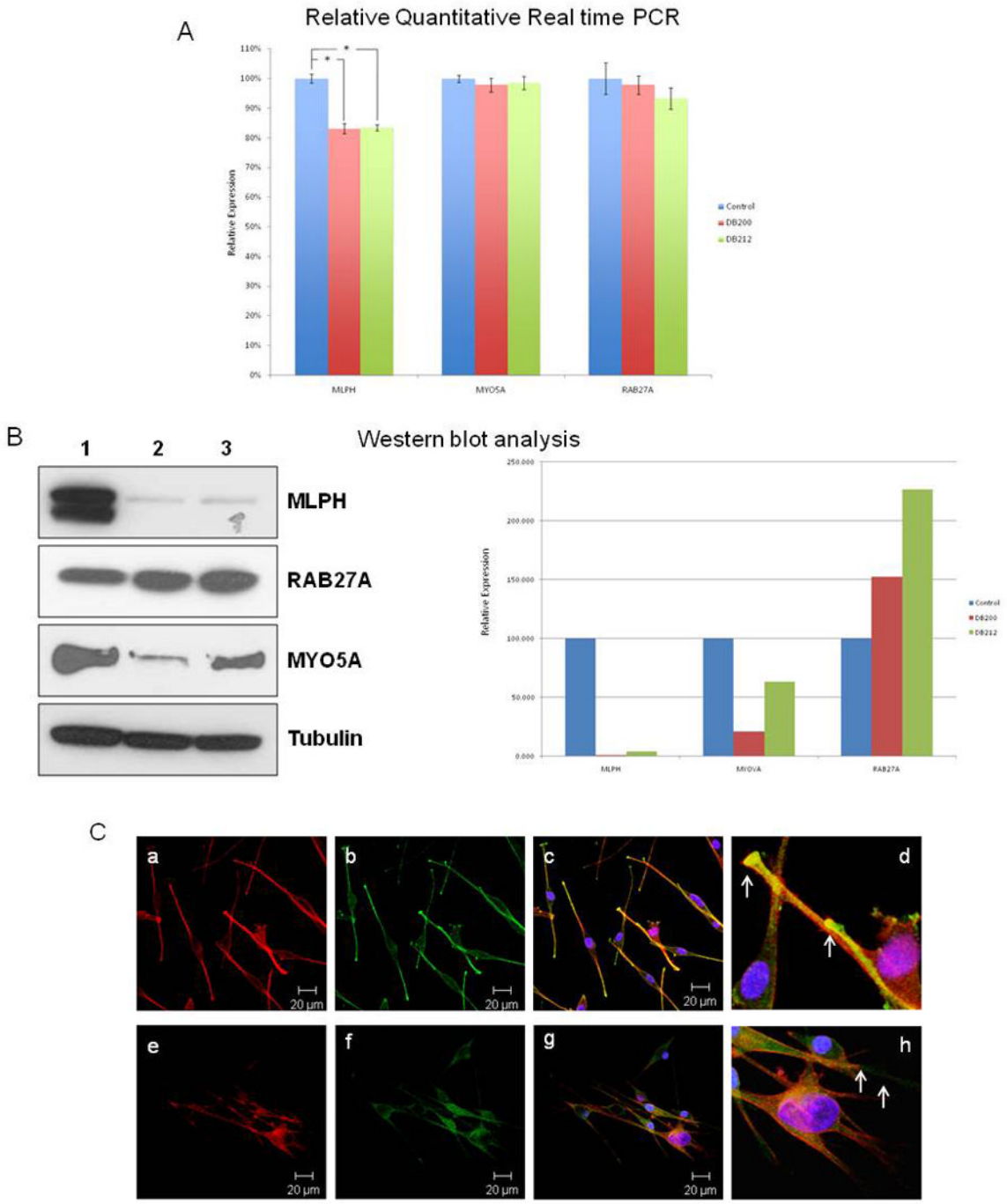

Figure 4. Endogenous mRNA and protein expression of MPLH, MYO5A and RAB27A in control and GSIII melanocytes

(A) Relative mRNA expression of *MLPH*, *MYO5A*, and *RAB27A* in control and patient cells. Values shown are mean values of expression normalized by *GAPDH* and relative to control, which is set to 100% for each gene. Errors bars represent ± 1 SEM, n=3 independent experiments and * denotes $p<0.001$ by two-tailed T-test. (B) Western blot analysis of protein extracts from control (lane 1), DB200 (lane 2) and DB212 (lane 3) melanocytes stained with antibodies to MYO5A, MLPH, RAB27A, and Tubulin (protein loading control). Both primary GSIII melanocytes cell lines expressed a significantly

decreased amount of MLPH protein, some decreased MYO5A and increased RAB27A proteins. (C) Control (a–d) and DB200 (e–h) melanocytes stained for actin (phalloidin-555; a,e) and MLPH (b,f). MLPH co-localized with actin in control melanocytes in the cell periphery and the dendritic tips (c, d arrows). In DB200 melanocytes, MLPH showed a faint diffuse distribution with minor co-localization with the actin-network (g, h arrows). Scale bar = 20 μm.

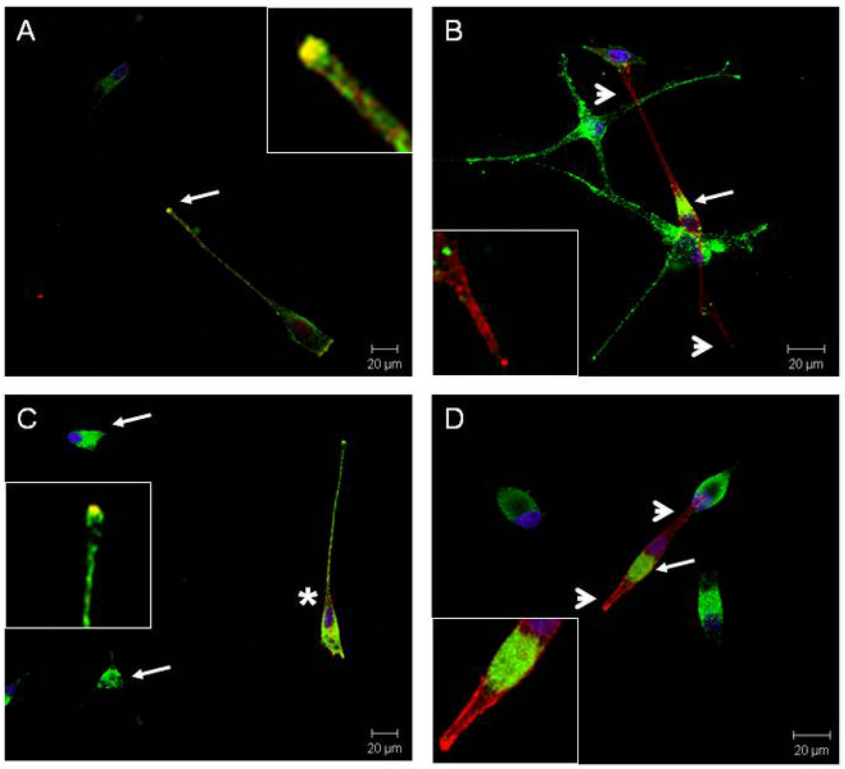

Figure 5. Distribution of melanosomes in control and GSIII melanocytes transfected with MLPH or MLPH(R35W)

Melanocytes electroporated with DsRed-MLPH(WT) (A, C) or DsRed-MLPH(R35W) (B, D) and co-stained with anti-mouse HMB45 antibodies (green) and nuclear stain (blue). (A) Control melanocytes electroporated with DsRed-MLPH(WT) (red) show a punctate peripheral distribution, accumulating with the melanosomal marker HMB45 (green) in the dendritic tips (arrow, insert). (B) Control melanocytes electroporated with DsRed-MLPH(R35W) show a peripheral distribution of DsRed (arrowheads) and induction of a perinuclear accumulation of HMB45 (green, arrow); dendrites and dendritic tips are nearly devoid of HMB45 (arrowheads, insert). (C) GSIII melanocytes electroporated with DsRed-MLPH(WT) (asterisk) rescued the HMB45 distribution from a perinuclear to a punctate peripheral distribution with co-localization of both MLPH and HMB45 (insert), while non-transfected melanocytes retained the perinuclear localization of HMB45 (arrows). (D) GSIII melanocytes electroporated with DsRed-MLPH(R35W) show a peripheral distribution of the mutant MLPH in the transfected cell (arrowheads), however the perinuclear localization of HMB45 (green, arrow) was not corrected (arrow, insert). Scale bars = 20 μm

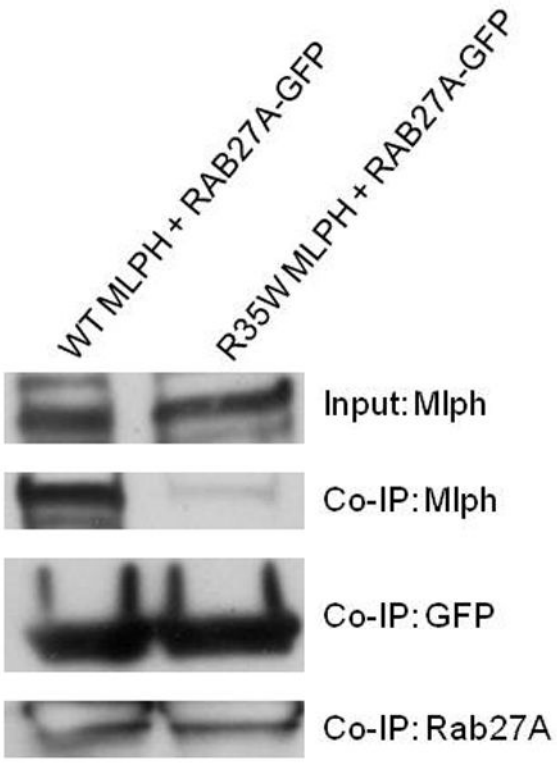

Figure 6. MLPH and MLPH(R35W) interactions with RAB27A

Co-immunoprecipitation (co-IP) on protein extracts from HEK cells transfected with GFP-RAB27A(WT) and DsRed-MLPH(WT) (lane 1) or DsRed-MLPH(R35W) (lane 2). The IP was performed with anti-GFP antibodies (lane 1 and 2). Total protein lysate (input) was stained with anti-MLPH (upper panel), co-IP lysate was stained with anti-MLPH, anti-GFP, and anti-RAB27A antibodies. GFP-RAB27A(WT) did pull down MLPH(WT) (lane 1) but only a small amount of mutant MLPH(R35W), despite equal amounts being present in the input lysate.

Table 1

Clinical manifestations of GSIII patients

Patient	Age (years)	Silver hair	Recurrent infections	Chronic lung disease	Neurological manifestations
DB212 *	14	yes	no	Since age 4	no
DB213	4	yes	no	no	no
DB252	19	yes	no	no	Psychomotor retardation
DB250	18	yes	no	no	no
DB200	4	yes	yes **	no	no
DB273	8	yes	no	no	no
DB275	19	yes	no	no	no

* marfanoid status

** recurrent pneumonia, hypogammaglobulinemia